ECOGRAPHY

Research

Comprehensive estimation of spatial and temporal migratory connectivity across the annual cycle to direct conservation efforts

Elly C. Knight, Autumn-Lynn Harrison, Amy L. Scarpignato, Steven L. Van Wilgenburg, Erin M. Bayne, Janet W. Ng, Emily Angell, R. Bowman, R. Mark Brigham, Bruno Drolet, Wendy E. Easton, Timothy R. Forrester, Jeffrey T. Foster, Samuel Haché, Kevin C. Hannah, Kristina G. Hick, Jacques Ibarzabal, Tara L. Imlay, Stuart A. Mackenzie, Alan Marsh, Liam P. McGuire, Gretchen N. Newberry, David Newstead, Andrea Sidler, Pam H. Sinclair, Jaime L. Stephens, David L. Swanson, Junior A. Tremblay and Peter P. Marra

E. C. Knight (https://orcid.org/0000-0002-8578-892X) ✉ (ecknight@ualberta.ca), E. M. Bayne and J. W. Ng, Dept of Biological Sciences, Univ. of Alberta, Edmonton, AB, Canada. – A.-L. Harrison, A. L. Scarpignato and P. P. Marra, Migratory Bird Center, Smithsonian Conservation Biology Inst., National Zoological Park, Washington, DC, USA. PPM also at: Dept of Biology and McCourt School of Public Policy, Georgetown Univ., Washington, DC, USA.– S. L. Van Wilgenburg, B. Drolet, W. E. Easton, S. Haché, K. C. Hannah, T. L. Imlay and P. H. Sinclair, Environment and Climate Change Canada, Canadian Wildlife Service, Saskatoon, SK, Canada. – E. Angell and R. Bowman, Avian Ecology Program, Archbold Biological Station, Venus, FL, USA. – R. M. Brigham and A. Sidler, Dept of Biology, Univ. of Regina, Regina, SK, Canada. – T. R. Forrester, Montana Cooperative Wildlife Research Unit, Univ. of Montana, Missoula, MT, USA. – J. T. Foster, Pathogen and Microbiome Inst., Northern Arizona Univ., Flagstaff, AZ, USA. – K. G. Hick and J. A. Tremblay, Wildlife Research Division, Science and Technology Branch, Environment and Climate Change Canada, QC, Canada. – J. Ibarzabal, Dépt des Sciences Fondamentales, Univ. du Québec à Chicoutimi, Chicoutimi, QC, Canada. – S. A. Mackenzie, Birds Canada, Port Rowan, ON, Canada. – A. Marsh, Lotek Wireless Inc., St John's, NL, Canada. – L. P. McGuire, Dept of Biological Sciences, Texas Tech Univ., Lubbock, TX, USA. – LPM and D. L. Swanson, Dept of Biology, Univ. of Waterloo, Waterloo, ON, Canada. – G. N. Newberry, Dept of Biology, Univ. of South Dakota, Vermillion, SD, USA. – D. Newstead, Coastal Bend Bays & Estuaries Program, Corpus Christi, TX, USA. – J. L. Stephens, Klamath Bird Observatory, Ashland, OR, USA.

Ecography
44: 665–679, 2021
doi: 10.1111/ecog.05111

Subject Editor: Cagan Sekercioglu
Editor-in-Chief: Miguel Araújo
Accepted 31 December 2020

Migratory connectivity is the degree to which populations are linked in space and time across the annual cycle. Low connectivity indicates mixing of populations while high connectivity indicates population separation in space or time. High migratory connectivity makes individual populations susceptible to local environmental conditions; therefore, evaluating migratory connectivity continuously across a species range is important for understanding differential population trends and revealing places and times contributing to these differences. The common nighthawk *Chordeiles minor* is a widespread, declining, long-distance migratory bird. Variable population trends across the nighthawk breeding range suggest that knowledge of migratory connectivity is needed to direct conservation. We used GPS tags to track 52 individuals from 12 breeding populations. We estimated migratory connectivity as 0.29 (Mantel coefficient: 0 = no connectivity, 1 = full connectivity) between the breeding and wintering grounds. We then estimated migratory connectivity at every latitude (spatial connectivity) or day (temporal connectivity) of migration and smoothed those migratory connectivity estimates to produce continuous migratory connectivity 'profiles'. Spatial and temporal connectivity were highest during migration through North America (around 0.3–0.6), with values generally around 0 in Central and South America due to mixing of populations along a common migratory route and similar migration timing across populations. We found local peaks in spatial and temporal connectivity during migration associated with crossing the Gulf of Mexico. We used simulations to estimate

NORDIC SOCIETY OIKOS

www.ecography.org

© 2021 The Authors. Ecography published by John Wiley & Sons Ltd on behalf of Nordic Society Oikos
This is an open access article under the terms of the Creative Commons Attribution License, which permits use, distribution and reproduction in any medium, provided the original work is properly cited.

the probability that our method missed peaks (spatial: 0.12, temporal: 0.18) or detected false peaks (spatial: 0.11, temporal: 0.37) due to data gaps and showed that our approach remains useful even for sparse and/or sporadic location data. Our study presents a generalizable approach to evaluating migratory connectivity across the full annual cycle that can be used to focus migratory bird conservation towards places and times of the annual cycle where populations are more likely to be limited.

Keywords: aerial insectivore, full annual cycle, migration, migratory connectivity, movement, population trend

Introduction

Conservation of migratory birds is complicated by the multitude of natural and anthropogenic factors influencing populations across their annual cycle. Research has focused on population pressures during the breeding season; however, the drivers of population declines can also occur during migration or on the wintering grounds (Marra et al. 2015). Those drivers can operate at the species level, affecting all populations similarly, or at the population level, resulting in differential regional trends (Cresswell 2014). Unfortunately, determining what drives population trends is limited by our ability to assess migratory connectivity across the annual cycle, particularly for migratory species with large geographic ranges.

Quantifying migratory connectivity (the degree to which populations are linked in space and time) across the annual cycle can facilitate understanding population trajectories and the factors influencing them (Webster et al. 2002, Marra et al. 2018). Migratory connectivity is high when individuals remain spatially separated into populations between seasons of the annual cycle and low when individuals from multiple populations mix (Fig. 1). When calculated between stationary stages of the annual cycle (i.e. breeding and wintering), migratory connectivity is due primarily to the spatial arrangement of individuals ('spatial connectivity'). During the migratory period, migratory connectivity is also influenced by how populations are separated across time ('temporal connectivity'; Bauer et al. 2016). Temporal connectivity can be caused by variation between populations in breeding ground departure and arrival timing (Gow et al. 2019), the timing of stopover (Cohen et al. 2018) or the rate of migration itself. High temporal connectivity results in spatial separation of populations, but only for a specific period of time (Fig. 1). It is therefore important to evaluate temporal as well as spatial connectivity because populations with low spatial connectivity at a particular location (e.g. migratory stopover) could have high temporal connectivity if individual populations migrate through that location at different times (Fig. 1; Bauer et al. 2016, Briedis et al. 2016, van Wijk et al. 2018).

Understanding migratory connectivity provides insights into population declines by identifying the places and times during the annual cycle that could be associated with differential population trends (Webster and Marra 2005, Marra et al. 2006, Cresswell 2014). When populations have high connectivity between periods of the annual cycle, each population is exposed to different local environmental conditions and thus the differences between population-specific vital rates may be more strongly influenced by those conditions. When populations have low connectivity, environmental conditions can affect vital rates at the species level (Cresswell 2014), particularly when individuals are constrained to a small area or time period ('bottleneck'; e.g. Isthmus of Panama, Bayly et al. 2018). Differentiating between the spatial and temporal components of connectivity is important for identifying potential causes of differential population trends because high spatial connectivity can cause differential trends via environmental conditions that vary in space (e.g. habitat loss); however, high temporal connectivity can only influence differential trends via factors varying in time (e.g. resource availability; Bauer et al. 2016).

If the objective is to understand differential population trends, then spatial and temporal migratory connectivity should be estimated range-wide and continuously (hereafter 'comprehensively') to avoid missing places and/or times during the annual cycle in which populations are most connected (Briedis et al. 2016). Estimating migratory connectivity during the migratory stages of the annual cycle is complex due to the number of locations that individuals occupy and the differences in timing of movements between populations. Migratory connectivity is thus typically estimated between stationary breeding and wintering ranges (Bauer et al. 2016, Cohen et al. 2017a), or occasionally between the breeding grounds and known migratory stopover locations (Cohen et al. 2018). These approaches may miss other locations or times of high migratory connectivity during the annual cycle, especially during migration, and so may fail to identify where populations experience conditions that explain differential trends (Briedis et al. 2016).

Using migratory connectivity to identify places and times that may drive differential population trends requires a range-wide approach because it can reveal patterns that are masked at regional scales (Koleček et al. 2016, Phipps et al. 2019). Some species show low connectivity at the regional scale, with high connectivity only revealed at the range-wide scale due to migratory divides (Finch et al. 2015, 2017, Hobson et al. 2015, Sarà et al. 2019). Sampling across the species' range also facilitates the inclusion of populations with varying population trends, which can be used to test specific hypotheses about factors driving those trends (Rushing et al. 2016).

We introduce a comprehensive approach to evaluating migratory connectivity that identifies places and times during the annual cycle with relatively high migratory connectivity and could explain differential population trends. Our goal was to continuously describe and identify peaks in spatial and temporal migratory connectivity across the annual cycle for a long-distance migratory bird, the common nighthawk *Chordeiles minor*. The common nighthawk would benefit

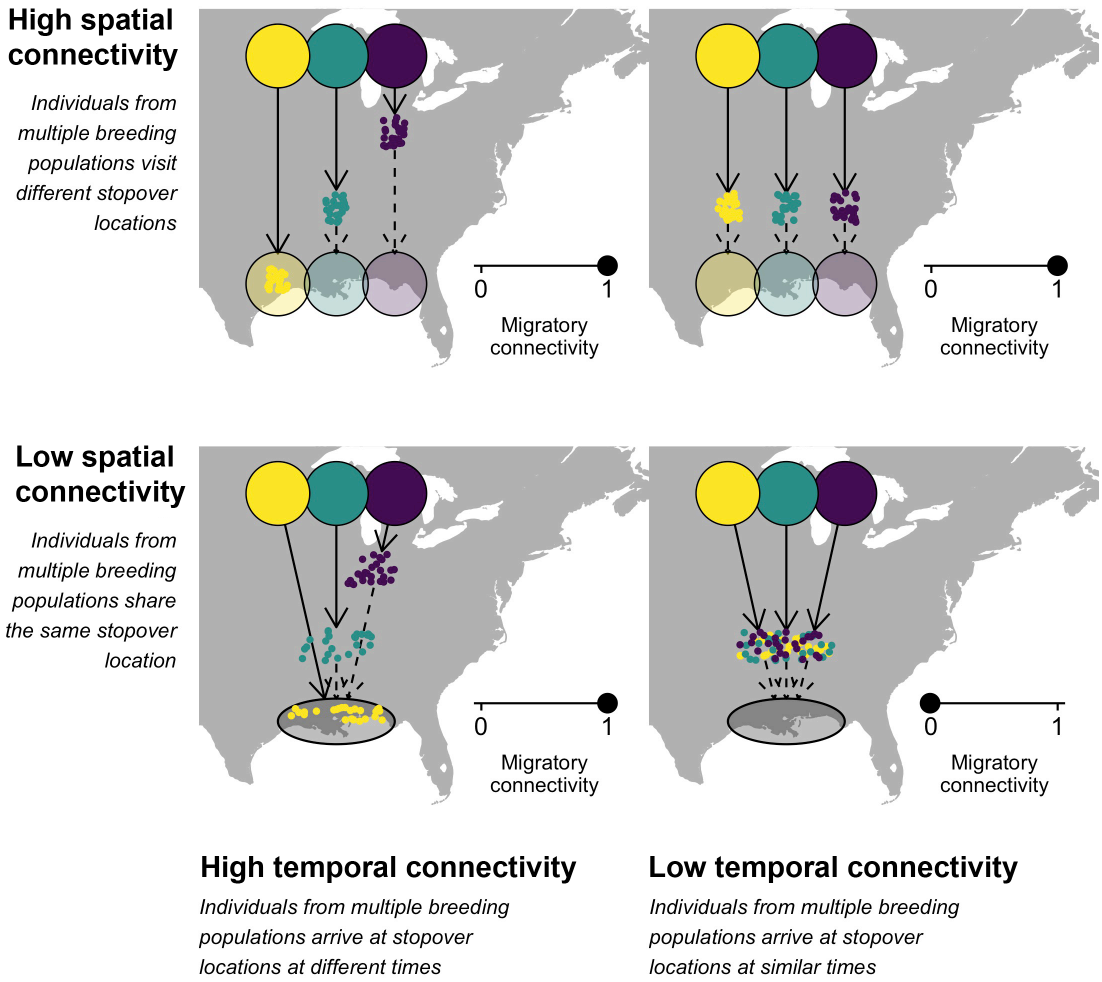

Figure 1. Theoretical snapshot of the spatial and temporal components of migratory connectivity during migration. Spatial and temporal connectivity combine to create high migratory connectivity (i.e. breeding populations are spatially separated) when either or both are high. The scale shown ranges from low (0) to high (1), although migratory connectivity can also be negative if individuals from breeding populations are further apart than random during migration. Opaque circles represent breeding areas of three distinct populations of a migratory bird, transparent circles represent a stopover location during migration, and dots represent individuals from each breeding population undertaking migration.

from a comprehensive evaluation to direct conservation efforts because a variety of mechanisms have been hypothesized for variable breeding population trends (−6.27 to 2.03% change per year, 1966–2015, Sauer et al. 2017) such as habitat loss on the wintering grounds and pesticide use at migratory stopovers (Brigham et al. 2011, Environment Canada 2016). We used GPS tags to track 52 common nighthawks from 12 breeding populations across the breeding range and estimated migratory connectivity during migration and the wintering season using the transmitted GPS data. We used the GPS data collected during migration to develop 'connectivity profiles' by estimating migratory connectivity at equally spaced intervals across the migration period using predictions from movement models. We constructed spatial (longitudinal) and temporal connectivity profiles for fall and spring migration and identified peaks in those profiles to identify places and times that could explain the differential population trends observed for common nighthawks. The GPS dataset we used had temporal gaps and unbalanced sampling due to battery limitations of the tags. To assess the impact of this, we conducted a simple migration simulation to determine the generalizability of our methods to different sample sizes.

Methods

GPS tag deployment

We selected thirteen locations across the common nighthawk breeding range to deploy GPS tags (Fig. 2). The locations were selected to sample the latitudinal and longitudinal gradients of the breeding range and the range of differential population trends reported for the species; therefore, we hereafter refer to them as 'populations'. We deployed 94 PinPoint GPS-Argos satellite tags (3.5 g) during the breeding seasons of 2015–2018 (Supporting information). PinPoint

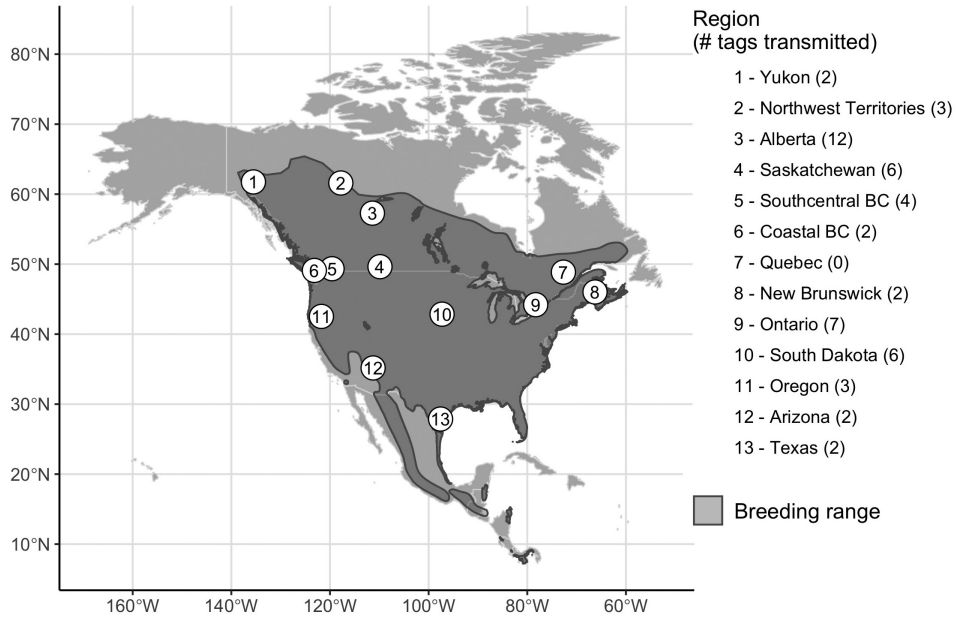

Figure 2. Location and quantity of GPS tags deployed on adult common nighthawks that successfully transmitted locations (excluding those that only transmitted from the breeding grounds or stopped moving/transmitting during migration).

GPS-Argos satellite tags collect GPS points and transmit the stored points via the Argos satellite system (Scarpignato et al. 2016). Tags deployed had different capacities due to different firmware versions; however, all schedules included at minimum one GPS point every 10 days between 10 August and 15 June (Supporting information).

Adult male and female nighthawks were caught through a variety of methods (Supporting information). Each captured individual was inspected and weighed prior to harness attachment to ensure it had no injuries and was large enough to carry the GPS tag (70–95.5 g, mean = 77.5 g, SD = 5.9 g; 3.5 g tag and harness ≤ 5% of body mass; Supporting information). Individuals weighing at least 70 g and with no injuries were fitted with a backpack-style harness (Åkesson et al. 2012; negligible mass < 0.05 g) made of 0.7 mm elastic plastic cord and aluminum crimp beads. We returned to most locations the year following deployment and attempted to retrieve the deployed tags to determine whether additional GPS points were stored on the tags but not transmitted via the Argos satellite system (Supporting information). We retrieved three tags by recapturing individuals and two tags through retrieval of roadkill carcasses; however, one roadkill bird died before the tag began its data collection schedule. We were unable to retrieve any tags that failed. All tracking data are stored in Movebank (Kranstauber et al. 2011) and are included in the Arctic Animal Movement Archive (Davidson et al. 2020).

Screening and processing of raw tracking data

We received GPS points from 61 of the 94 deployed GPS tags. Those tags collectively transmitted 2001 GPS points, 653 of which we removed because they failed the manufacturer's check for accurate transmission (Lotek Wireless Inc.; Supporting information). The four tags that we retrieved contained an additional 154 GPS points (range: 17–51 per tag) that did not transmit via the Argos satellite system. Prior to further analysis, we inspected the GPS points for each individual in a geographic information system (GIS) to identify and remove data for nine tags from the dataset: two only transmitted from the breeding grounds and seven stopped moving or transmitting during migration. At least one tag transmitted data for all populations except Quebec. This resulted in a final dataset of 52 birds from 12 populations (10 female, 42 male).

We assigned each GPS point to a season of the annual cycle (breeding, fall migration, wintering, spring migration). We defined breeding points for the year of deployment and the following year as all points within 100 km of the capture location (Ng et al. 2018), with the exception of one individual who returned to a territory 125 km northeast of its capture location. We defined wintering season points as all points within 100 km of the point furthest from the capture location and defined wintering grounds as at least two wintering season GPS points within 100 km of another. Manual review suggested that seven individuals relocated to a second area during the wintering season; we defined those second wintering areas as at least two consecutive GPS points within 100 km of each other but more than 100 km from the first wintering area and spanning a period of at least three weeks (to differentiate from stopovers; maximum two weeks). We then assigned all remaining points to the appropriate migration season.

We used linear mixed effects models to test the classified data for evidence of differential migration that could affect subsequent migratory connectivity analyses (methods and results in the Supporting information). On average, females

wintered farther west than males at the beginning of the season; however, this was driven by one female that wintered farthest west (Supporting information). There was no difference in wintering longitude between males and females after seven males relocated wintering territories partway through the season (null model ΔAICc = 0.00). Females migrated farther west and later than males during spring migration; but this was likely an artifact of our small sample size for females during spring migration (n = 6), which were primarily from the western populations that have later spring migration arrival timing (Fink et al. 2020). We therefore did not separate our analyses by sex. We found no effect of deployment year on migration timing (all models > Δ2 AICc from selected model).

Data screening and processing was conducted in R ver. 3.5.2 (<www.r-project.org>) with the geosphere (Hijmans 2017) and lme4 (Bates et al. 2015) packages. Distances were calculated as Haversine great circle distance.

Continuous-time predictions of individual location

Our dataset had temporal gaps and unbalanced sampling due to limited battery capacity and imperfect tag performance, which is common to movement datasets collected from small and medium-sized migratory birds. These gaps impede comprehensive evaluation of spatial and temporal connectivity during migration because individual locations are unknown for some periods along the migration route. We filled in the gaps in our dataset by using continuous-time correlated random walk (CRAWL) models (Johnson et al. 2008) to interpolate the migration path for each individual. We chose CRAWL for four reasons. First, CRAWL incorporates inertia via a correlated random walk, which is particularly important during directional movement such as migration. Second, the continuous-time nature of the model accommodates irregularly spaced gaps in data collection. Third, the model provides spatially and temporally explicit predictions, allowing us to estimate both spatial and temporal connectivity (next section). Fourth, CRAWL provides an estimate of prediction uncertainty that can be incorporated in migratory connectivity estimations.

We only constructed movement models for individuals with sufficient sampling across the migration period because predicted movement path can be affected by GPS sampling intensity (Rowcliffe et al. 2012). We first attempted to define sufficient sampling using a threshold; however, there was a linear relationship between inter-point duration and distance travelled, suggesting no effect of sampling intensity on distance between points. We therefore included all individuals that had 1) a known wintering site, 2) at least one point in each of North, Central and South America and 3) at least one point on either side of the Mississippi region where birds congregate during fall migration before turning south (to ensure movement path accuracy in this potentially important stopover area).

We used the CRAWL package (Johnson et al. 2008, Johnson and London 2018) in R to construct four sets of movement models, the results of which comprised a mean predicted migration path and standard error for each individual (Supporting information). For each migratory season (fall, spring), we constructed one set of models with an emphasis on the spatial predictions of the model (to evaluate spatial connectivity), and one set of models with an emphasis on the temporal predictions of the model (to evaluate temporal connectivity). We included the capture location and the wintering location as known points in the spatially-focused models; however, we excluded them from the temporally-focused models because they did not have dates associated with them and thus would introduce inaccuracy into estimates of temporal connectivity. The temporal resolution of our data did not allow us to define behavioural classes during migration such as stopover and migration flight, so we assumed constant migratory movement in the model. We extracted the locations of each individual's mean predicted migration pathway from their fitted movement model at every latitude for the spatially-focused models and every day for the temporally-focused models.

Connectivity estimation

Breeding to nonbreeding connectivity

We quantified connectivity using the Mantel test (r_M; Ambrosini et al. 2009, Cohen et al. 2017b), which estimates the correlation between two distance matrices. The Mantel correlation coefficient ranges from −1 to 1, with 1 indicating that individuals from each population stay together between seasons, 0 indicating complete mixing of populations between seasons, and 1 indicating that individuals close to each other in one season are further apart during the other season.

We estimated connectivity relative to the breeding grounds because our goal was to inform potential causes of differential population trends observed on the breeding grounds. We only used data from individuals for which there were at least two wintering season GPS points within 100 km of another (n = 43). We defined the breeding location for each individual as the capture location. We then incorporated uncertainty in the wintering location by estimating the Mantel coefficient using a bootstrapping approach. First, we calculated the standard deviation of the wintering points for each individual, then we randomly sampled from a normal distribution with that standard deviation, added that sampled location error to the mean wintering location for that individual, and calculated r_M of the resultant coordinates. We repeated the process 1000 times to estimate connectivity between the breeding and wintering grounds. We repeated this process twice; once using the first wintering area for all individuals, and once using the second wintering area for those individuals that relocated during the winter (n = 7).

Migration – spatial connectivity

We estimated spatial connectivity separately for fall and spring migration. To continuously evaluate spatial connectivity across the migratory period, we used the spatially-focused predicted migration paths to estimate r_M at each degree

latitude of migration. We estimated r_M at all latitudes for which CRAWL predicted locations for at least three individuals from two populations (fall: 58°N to 16°S; spring: 58°N to 14°S) using the same methods described above (breeding to nonbreeding connectivity), except that we incorporated uncertainty from the movement models by including the mean standard error of the location predictions as the location error instead of the standard deviation of wintering points.

Migration – temporal connectivity

We repeated the spatial connectivity methods, but instead used the temporally-focused movement paths to estimate r_M for every day of migration. We used all dates for which there were location predictions available for at least three individuals from two populations (fall: 20 August to 21 November; spring: 22 February to 11 June).

Migration connectivity profiles

We used generalized additive models (GAMs, Wood 2017) from the mgcv package (Wood 2011) in R to smooth the r_M estimates for fall and spring migration into continuous spatial and temporal migratory connectivity (hereafter 'connectivity profiles'). We chose GAMs because we expected multiple peaks in the connectivity profiles and GAMs can model complex, nonlinear patterns by averaging multiple regressions with varying coefficients. For each profile, we fit a Gaussian GAM with a cubic spline smoother with shrinkage to the bootstrapped r_M estimates with latitude (spatial profiles) or day (temporal profiles) as the predictor variable. We determined the number of knots in the GAM as the minimum number between 5 and 15 that best fit within the 99% CI of the r_M estimates (fall spatial: 14 knots, spring spatial: 15 knots, fall temporal: 15 knots, spring temporal: 15 knots).

Peak identification

We interpreted local maxima (hereafter 'peaks') in the connectivity profiles to represent places and times that could drive differential population trends because of elevated spatial–temporal connectivity. For each of the four connectivity profiles, we automatically identified all peaks in the mean prediction of the GAM for each profile using the pracma package (Borchers 2019). For peaks that were within five degrees latitude or ten migration days of each other, we assumed these were associated with the same general place or time and used only the highest peak.

We used a two-step process to validate each peak. The first was a leave-one-out analysis, much like jackknife resampling (Efron and Stein 1981), that checked for bias in the global connectivity profile. For the spatial connectivity profiles, we removed one population, re-estimated r_M at each latitude, and fit a GAM to the resultant data. We repeated the process for each population and used mean shift classification with a bandwidth of two in the meanShiftR package (Lisic 2018) to cluster the peaks from all iterations into groups based on latitude and r_M. This leave-one-out process allowed us to differentiate between two types of peaks in the spatial connectivity profiles: 1) peaks due to an increase in connectivity during migration (i.e. a place of interest) were present in all leave-one-out-iterations; and 2) peaks due to the addition or removal of individuals from the r_M estimations as the connectivity profile moved across the latitudinal gradient of the breeding grounds (i.e. a sampling artifact) were absent in at least one leave-one-out-iteration. Thus, we retained clusters that contained a peak from every leave-one-out iteration and removed clusters that classified as sampling artifacts. We used the same approach for the temporal connectivity profiles, except that instead of removing populations, we removed groups of individuals that 'started' or 'ended' migration on dates when the number of individuals in the analysis changed (i.e. scheduled GPS point days that followed the start or end of migration for the individuals included in the analysis).

For the second step, we assessed the remaining peaks using the confidence intervals of the r_M bootstraps. Peaks for which the 83.4% confidence interval (Krzywinski and Altman 2013) overlapped with the confidence intervals of both of the nearest local minima were not considered statistically significantly different from those minima.

Sample size simulation

Finally, we used a simulation to investigate the generalizability of our approach. We were specifically interested in the effects of sampling intensity (i.e. how many locations and individuals were included in analyses) on the probability of detecting true and false peaks in the connectivity profiles, and on the magnitude of r_M. We simulated the southward migration of three populations from the breeding grounds in Canada, migrating through a shared stopover with low spatial and temporal connectivity, through a second stopover with high spatial and temporal connectivity, and then arriving on the wintering grounds in Central America with low spatial and temporal connectivity (Fig. 3). We randomly varied the number of individuals sampled per population (2–20) and number of locations per individual (5–50) for 1000 iterations.

We populated the simulation by randomly selecting locations and dates for each individual in the simulation for each stage (breeding, two stopovers, wintering). The locations were randomly selected from a uniform distribution within a predefined area for each stage (Fig. 3). We simulated high spatial connectivity by first randomly selecting three population centroids within the breeding and second stopover stage areas, and then randomly selecting individual locations within 50 km of those centroids. The breeding centroids were required to be at least 500 km apart and the second stopover centroids were required to be at least 300 km apart. The dates were also randomly selected for each individual from uniform distributions for migration start date (1–20 days) and the time it took to travel between each stage (20–30 days). We

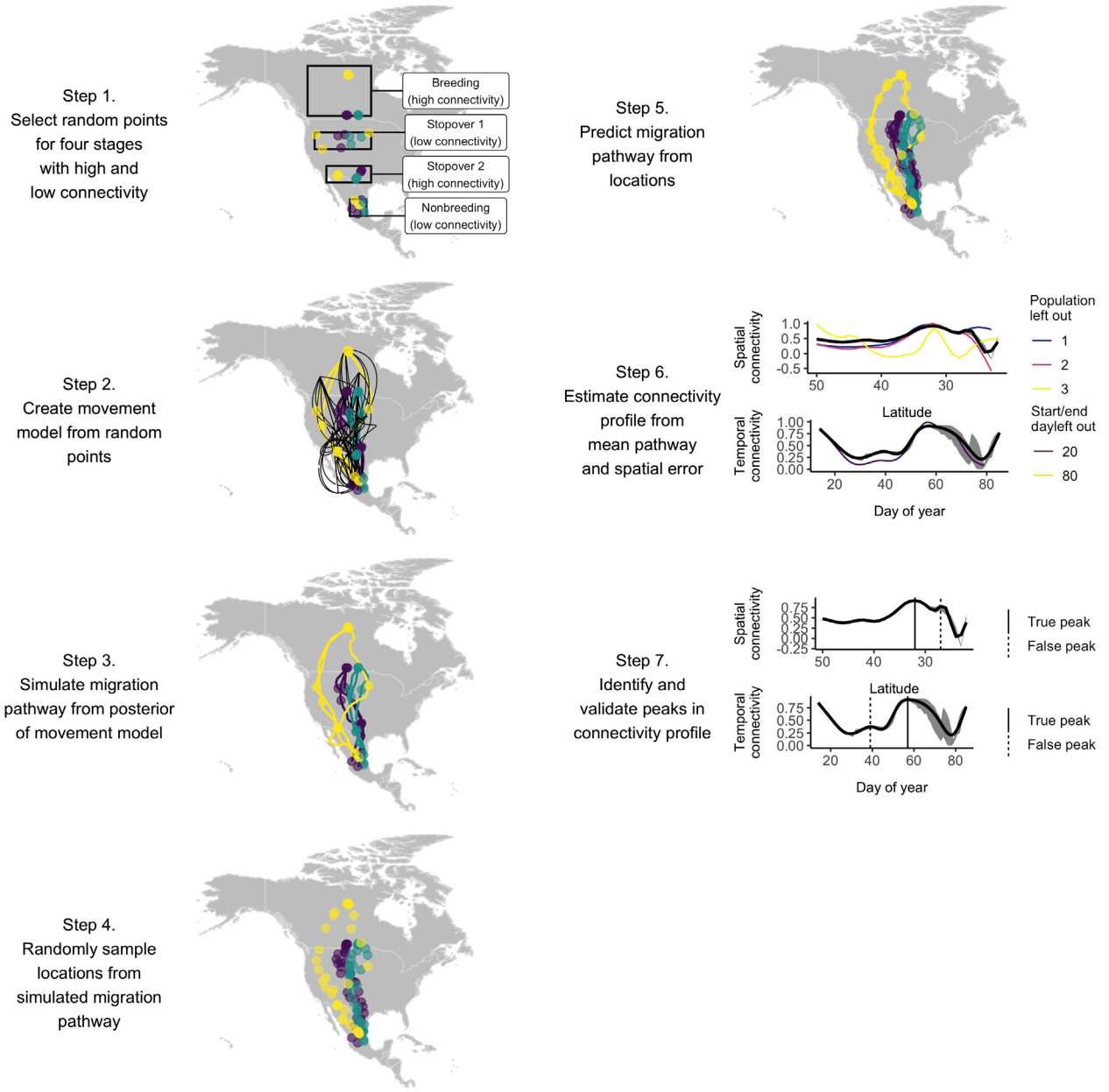

Figure 3. Example workflow of simulation to investigate the potential for false or missed peaks in connectivity profiles. Example shows the southward migration of three populations represented by different colors, with three individuals sampled per population and ten GPS points sampled per individual. Black lines in step 2 represent the standard error of the correlated random walk movement model for each individual.

simulated high temporal connectivity by selecting the dates for breeding ground departure and the second stopover at the population level instead of at the individual level.

We then fit a CRAWL movement model to the four points for each individual and used the posterior from the model to simulate a migration pathway for that individual. We randomly sampled between 5 and 50 locations from those simulated migration pathways to simulate GPS sampling for each individual. We applied our spatial and temporal connectivity profile methods (sections Continuous-time predictions of individual location, Connectivity estimation, Migration connectivity profiles, and Peak identification) to the simulated locations, with the exception that we generated 100 r_M estimates for each latitude or day, instead of 1000.

We classified the peaks identified in each simulation iteration as true positive or false positive by comparing it to where or when the peak was simulated at the second stopover (spatial connectivity: within 5° of the mean latitude across populations; temporal connectivity: within 10 days of the mean day across populations). We also classified the iterations for which no peaks were identified as false negatives. We then used logistic regression to model the probability of a false

positive relative to the number of individuals and number of GPS points per individual. We similarly modelled the probability of a false negative. We also used linear regression to test whether the value of r_M and the 95% CI of r_M were influenced by the number of individuals and the number of locations.

Results

Migration route

Common nighthawks from across the breeding range used a shared route for much of both migrations (Fig. 4). In fall, individuals migrated towards the Central/Mississippi flyway and flew south across the Gulf of Mexico. There was no indication of over-land migration through Mexico. All individuals then funneled along a narrow route in the Colombian Andes and continued across the Amazon basin towards their wintering grounds, mostly to the east in the Amazon and Cerrado biomes of Brazil (Fig. 5). In spring, individuals headed north and departed for the Gulf of Mexico from northern Colombia. After reaching the Gulf coast, each individual migrated back to its breeding grounds in North America.

Nonbreeding connectivity

r_M of breeding populations on the wintering grounds was 0.292 (0.291–0.293 95% CI; Fig. 5) at the beginning of the wintering season and decreased to 0.197 (0.195–0.198 95% CI) after some birds relocated to secondary wintering areas (7 of 43 individuals).

Fall migration connectivity

Mean spatial r_M of all bootstraps was 0.208 (0.022–0.395 95% CI) during fall migration. Spatial r_M started at 0.842 (0.764–0.967 95% CI) in the north at 58°N, quickly decreased to 0.405 (0.036–0.781 95% CI) at 54°N and stayed between 0.3 and 0.4 until 24°N as birds crossed the Gulf of Mexico (Fig 4). Mean spatial r_M then decreased to between 0.1 and −0.1 until 8°S when there were few individuals left in the analysis, and eventually reached −0.165 (−0.996 to 0.996 95% CI) at 16°S. There were no peaks in spatial connectivity during fall migration. The GAM fit to the bootstrapped r_M estimates explained 66.2% of the variation in the data.

Mean temporal r_M of all bootstraps was 0.138 (0.055–0.212 95% CI) during fall migration. Similar to spatial r_M, we found temporal r_M started relatively high at 0.630 (0.630–0.630 95% CI) on 20 August at the beginning of fall migration, but consistently decreased to approximately zero on 20 September (Fig. 4). Temporal r_M then stayed between 0 and 0.1 until one peak of 0.167 (0.131–0.181 95% CI) on 24 October after birds crossed the Gulf of Mexico (Fig. 6). Temporal r_M decreased to approximately zero when migration ended for most birds in mid-November. The three other peaks in fall temporal r_M on 10 September, 2 October and 16 November were identified as false peaks because they were not present in all leave-one-out iterations. The GAM fit to the bootstrapped r_M estimates explained 74.9% of the variation in the data.

Spring migration connectivity

Mean spatial r_M of all bootstraps was 0.100 (−0.042 to 0.293 95% CI) during spring migration. Spatial r_M started negative at −0.878 (−1.00 to −0.602 95% CI) in the south at 14°S and quickly increased to near zero before rising to a peak of 0.233 (0.040–0.421 95% CI) at 6°N in northern South America (Fig. 4). Spatial r_M dropped to zero until approximately 26°N during crossing the Gulf of Mexico. Spatial r_M then steadily increased as birds took direct routes back to their breeding grounds in North America, with another peak of 0.579 (0.348–0.744 95% CI) at 44°N in the northern United States where multiple populations veered off towards their breeding grounds. One false peak at –9°S was detected. The GAM fit to the bootstrapped r_M estimates explained 71.3% of the variation in the data.

Mean temporal r_M of all bootstraps was 0.064 (−0.243 to 0.351 95% CI) during spring migration. Temporal r_M began at 0.467 (−0.926 to 1.000 95% CI) on 22 February at the beginning of spring migration, before decreasing to near 0 as more birds initiated migration (Fig. 4). Temporal r_M then increased gradually to a peak at 0.256 (0.217–0.280 95% CI) on 7 May as birds crossed the Gulf of Mexico (Fig. 6). There was a steep increase in r_M until 25th May followed by a sharp decline before temporal r_M ended at −0.676 (−0.676 to −0.676 95% CI) on 11 June; however, this peak on 25 May was identified as false because it was not present in all leave-one-out iterations. Two other peaks on 2 and 25 March were not retained because the confidence intervals overlapped with adjacent minima. The GAM fit to the bootstrapped r_M estimates explained 55.9% of the variation in the data.

Sample size simulation

The rate of false negative (i.e. missed) peaks was 11.7% in the simulated spatial connectivity profiles and 18.7% in the simulated temporal connectivity profiles. The probability of detecting a true positive spatial peak was positively affected by the number of individuals sampled per population ($p < 0.001$) and the number of locations sampled per individual ($p = 0.013$; Fig. 7). The probability of detecting a true positive temporal peak was positively affected by the number of locations sampled per individual ($p = 0.006$), but not by the number of individuals sampled per population ($p = 0.067$). The rate of false positive (i.e. false) peaks was 10.8% in the simulated spatial connectivity profiles and 36.5% in the simulated temporal connectivity profiles. Visual inspection of these false positives showed that they were additional times of high connectivity, either near the beginning of migration (latitude 40–55°N, day 10–25) when connectivity was simulated as high or introduced by the stochasticity of the migration path simulation process. The probability of detecting a false positive spatial peak was negatively affected by the number

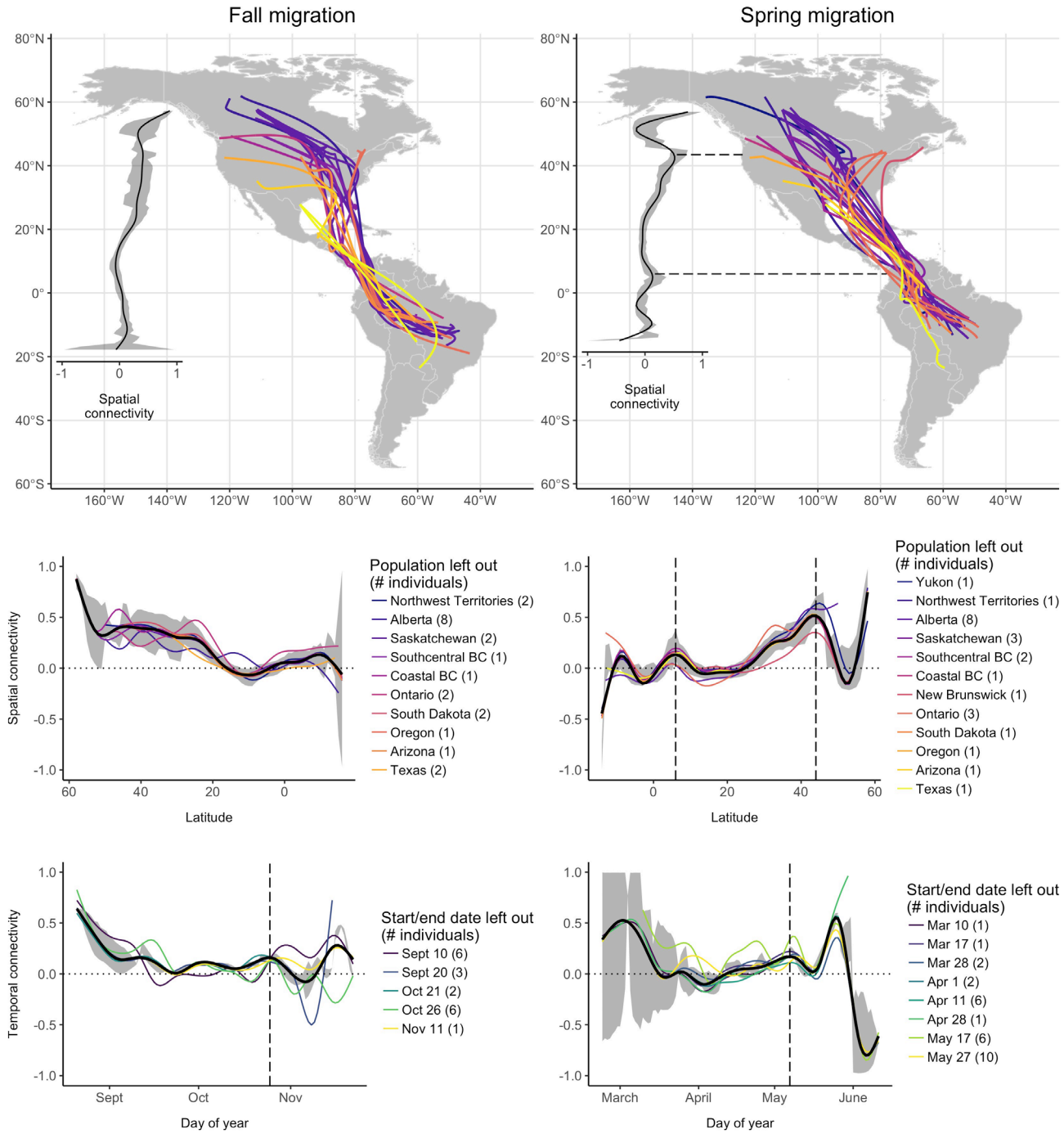

Figure 4. Migratory connectivity of adult common nighthawks during fall (left) and spring (right) migration. Top: colored lines are the mean predicted migration paths from correlated random walk movement models for each individual included in the analysis. Spatial connectivity profile on the left of each map is latitudinally aligned with the map (below for description of connectivity profile). Center (spatial connectivity profile) and bottom (temporal connectivity profile): The grey ribbon is the 83.4% CI of 1000 bootstraps of migratory connectivity (r_M) estimates at each latitude or day of year. The black line is the mean prediction from a generalized additive model (GAM) of those r_M estimates. Colored lines on the connectivity profiles are the mean prediction from a GAM of r_M estimates with one population or start/end date left out of the r_M estimation (i.e. jackknifed). Dashed lines represent local maxima that are considered true elevations in migratory connectivity. Local maxima that were not present in all jackknifes are attributed to changes in the population composition and thus are not biologically meaningful. Note that the spatial and temporal connectivity profiles do not correspond spatially in the figure.

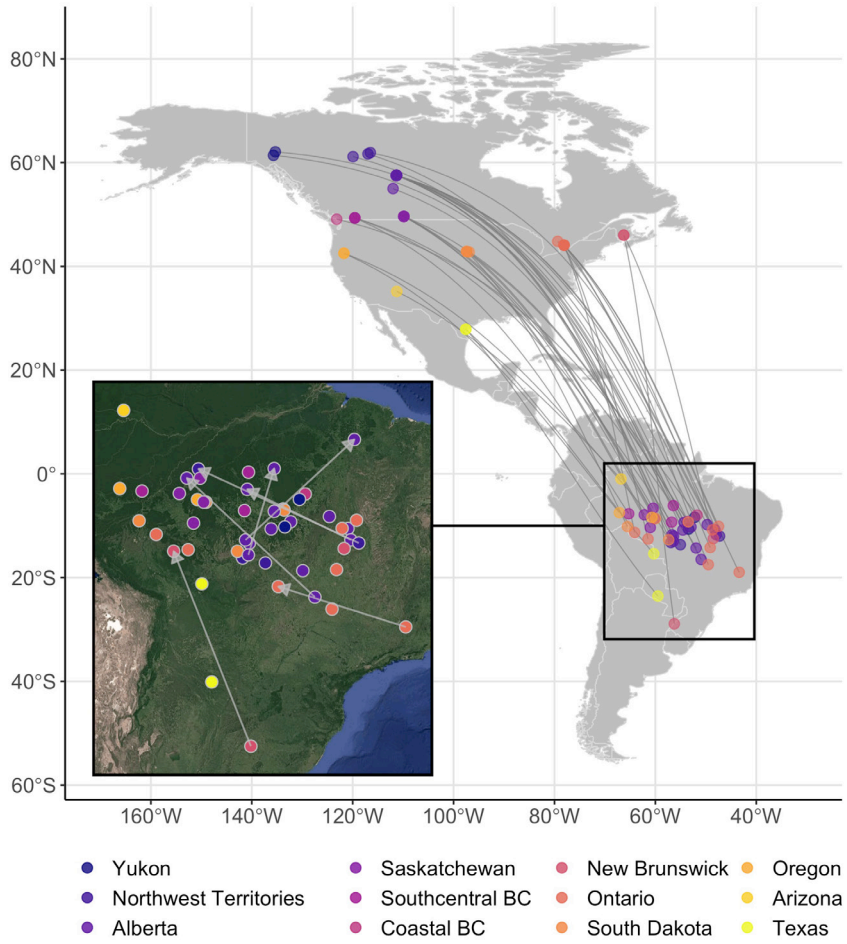

Figure 5. Great circle connections between adult common nighthawks on the breeding grounds in North America and wintering grounds in South America, as determined with Pinpoint GPS-Argos tags. Inset shows relocations of individuals that used two wintering areas during the wintering season.

of individuals sampled per population ($p = 0.008$) and the probability of detecting a false positive temporal peak was positively affected by the number of locations sampled per individual ($p = 0.026$). All other effects were non-significant ($p > 0.05$). The value of r_M ranged from −0.163 to 0.973 (mean = 0.500, SD = 0.237) for true positive spatial peaks and from −0.062 to 0.987 (mean = 0.581, SD = 0.213) for true positive temporal peaks. There was no effect of number of individuals per population or number of locations per individual on r_M of spatial or temporal peaks ($p = 0.05$), but there were highly significant effects of both predictors on the 95% CI of r_M ($p < 0.001$).

Discussion

Migratory connectivity provides insight into multiple aspects of a species' biology including where and when in the annual cycle breeding populations may be limited (Norris and Marra 2007, Cresswell 2014, Rushing et al. 2016). We comprehensively examined spatial and temporal connectivity across the annual cycle of the common nighthawk using a novel approach. We found low spatial connectivity outside of the breeding grounds due to the use of a single route for much of this species' spring and fall migration and mixing of populations on the wintering grounds, primarily in the Amazon and Cerrado biomes of Brazil. There were, however, places and times during migration when connectivity was elevated, indicating increased separation of populations in space and/or time. We discuss the generalizability of our approach and how it can guide future conservation efforts.

Quantifying migratory connectivity is a powerful tool for directing conservation research because it can be used to identify potential causes of differential population trends associated with times and places of the annual cycle with disproportionately high connectivity (Norris and Marra 2007, Cresswell 2014, Rushing et al. 2016). As with many species, the list of potential causes of decline for the common nighthawk is lengthy (Environment Canada 2016). During spring migration, we found a peak in spatial migratory connectivity in the northern Amazon region, which could create population-specific pressures through threats like habitat loss (Bayly et al. 2018) and pesticide use (Spiller and Dettmers 2019). We found increased population-specific timing of

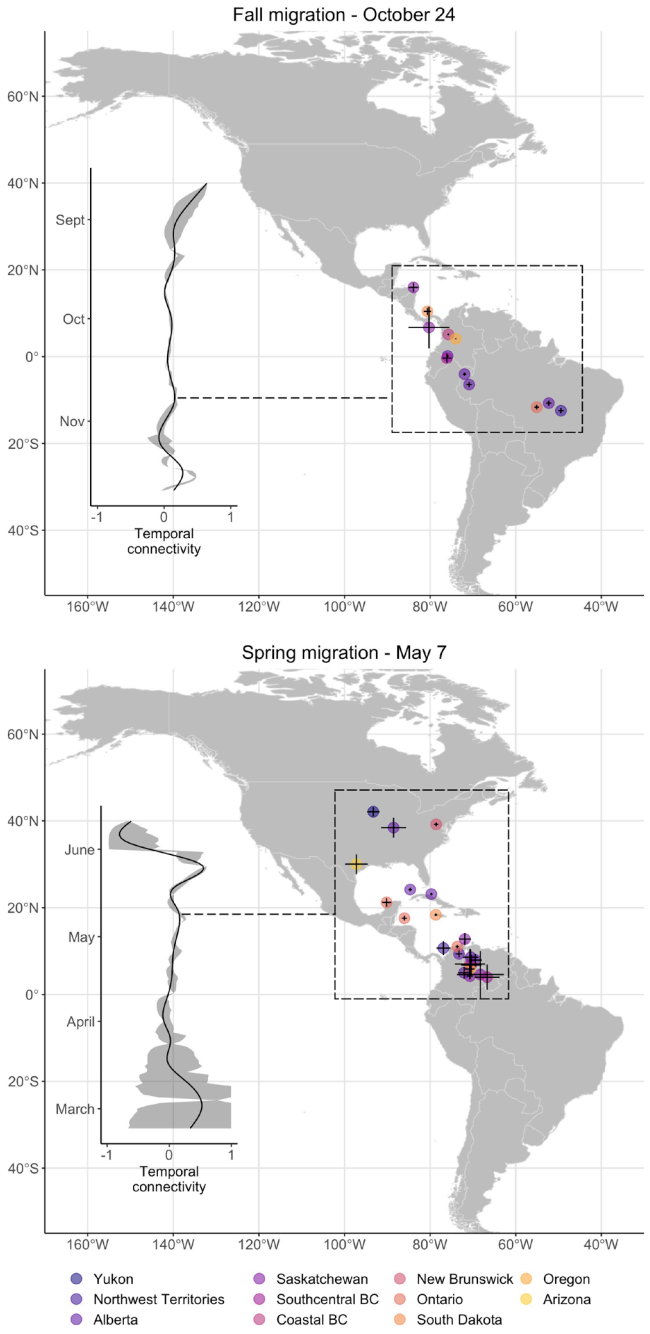

Figure 6. Locations of adult common nighthawk individuals during local maxima in temporal migratory connectivity during migration. Error bars on each location point represent the standard error at that location from correlated random walk movement models.

spring crossing of the Gulf of Mexico beginning 7 May, which could make individual populations vulnerable to temporally variable pressures like favorable winds (Bauer et al. 2016, Ries et al. 2018). We also found increased population-specific timing while birds were entering the Amazon basin on fall migration, but the magnitude of this peak was low (r_M=0.167). In North America, we found moderate (r_M=0.3–0.4) spatial connectivity north of the Gulf of Mexico during both migrations, which could affect breeding populations through threats like vehicle collisions in areas of high road density (Camacho 2013). We similarly found moderate fall and spring temporal connectivity in North America, suggesting population-specific breeding ground departure and arrival timing that could lead to differential population trends via threats like differential changes in aerial insect phenology (English et al. 2018). Finally, we found a strong peak in spatial connectivity at 44°N during spring migration. However, it is unclear whether this peak is a sampling artifact that was not detected by our leave-one-out analysis because it is attributed to multiple populations, or whether it represents a true spring migratory divide between eastern and western common nighthawk populations; further sampling is needed.

Connectivity profiles do not rule out potential threats on the breeding grounds like habitat change, drought or reduced insect abundance (English et al. 2017, Sánchez-Bayo and Wyckhuys 2019) if they are estimated relative to the breeding grounds. We also emphasize that the link between migratory connectivity and population trend applies only to differential population trends; other approaches are required to understand drivers of population decline occurring at the species level (Cresswell 2014). For example, recent land use change in the Magdalena River Valley of Colombia (Rodríguez Eraso et al. 2013) is unlikely to be responsible for differential population trends because all populations migrate together through this small area. Instead, this area represents a migratory bottleneck where mortality events or physiological stressors could negatively affect nighthawk population trends at the species level. Overall, low spatial and temporal migratory connectivity in South America suggests that the drivers of differential common nighthawk population trends are most likely in North America, but a sharp peak in spring spatial connectivity suggests drivers could also occur in northern South America before birds cross the Gulf of Mexico (Bayly et al. 2018).

Connectivity profiles can contribute to conservation of many migratory species because they are generalizable. Constructing connectivity profiles can be applied to a wide range of tracking data types (e.g. geolocator, Argos) because it accommodates uncertainty in location estimates. Further, connectivity profiles can be effectively derived from sparse datasets; the probability of detecting a true peak was almost 85% for spatial connectivity and 75% for temporal connectivity with as little as two individuals sampled per population and five locations sampled per individual. We did, however, find that the confidence interval of the connectivity profiles was highly affected by number of individuals and locations, which could affect the probability of detecting a peak in situations with moderate connectivity as opposed to our simulation of high connectivity. Although the application of temporal connectivity profiles to sparse and/or sporadic datasets such as ours results in large confidence intervals that may obscure conclusions, understanding temporal connectivity is a critical component of evaluating the causes of differential population trends. Connectivity profiles are a good first step towards conservation planning for the common nighthawk

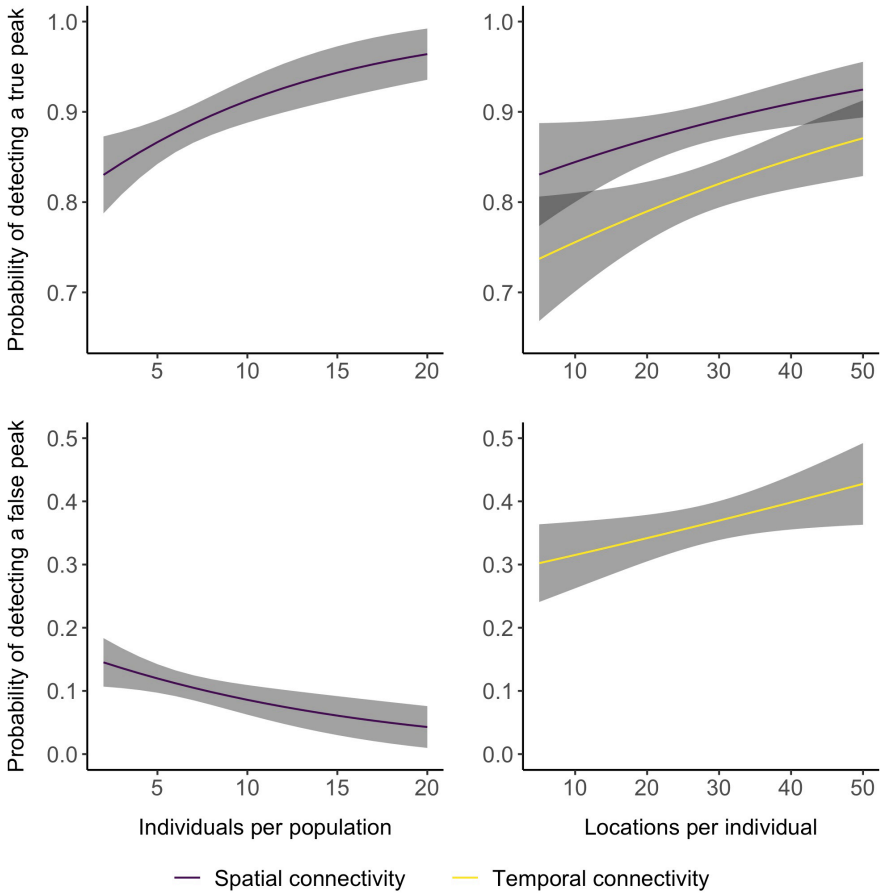

Figure 7. Probability of detecting a true or false peak in migratory connectivity using connectivity profiles depending on number of individuals sampled per population (n = 3 populations) and number of locations sampled per individual. Only significant effects are shown (alpha = 0.05).

and potentially other species. As tracking technology continues to improve, higher resolution datasets can be used to understand temporal connectivity with greater precision.

Although connectivity profiles are generalizable to many datasets, certain situations may increase the probability of false positive and negative peaks. First, our approach assumes constant migratory movement, which is a relatively safe assumption for an aerial insectivore like the common nighthawk that likely employs an energy-minimizing migration strategy (Imlay et al. 2020); however, time-minimizing migrants make extensive stopovers during migration (Alerstam and Hedenström 1998). Assuming constant migratory movement for those species would likely increase the probability of missing a peak in temporal connectivity because it would reduce the temporal clustering of individuals. Assuming constant movement would likely also increase the probability of detecting a false temporal peak, as our simulation revealed that temporal connectivity profiles are sensitive to stochastic times of high connectivity and the temporal resolution of location sampling. We therefore recommend higher temporal sampling (e.g. one location sampled per day) for species known to make extensive stopovers and differentiating between stopover and migration in the movement modelling prior to construction of connectivity profiles. Differential migration between years could mask or distort the temporal or spatial pattern of migration and increase the probability of missing a peak in connectivity. Differential migration between sexes can also exacerbate the effects of local environmental conditions on population dynamics (Briedis and Bauer 2018). We recommend testing for differential migration before constructing connectivity profiles and to construct separate profiles for each sex or year if differential migration is present. A small sample size for females and a potential confound between sex and an east–west gradient in spring migration (Fink et al. 2020) timing prohibited us from constructing separate profiles for male and female common nighthawks; however, we recommend that future conservation research consider potential for sex-specific population pressures during spring migration.

Interpretation of the magnitude of connectivity values remains an obstacle towards understanding migratory connectivity. Migratory connectivity is often referred to as 'low' or 'weak' and 'high' or 'strong' (Webster et al. 2002), and Finch et al. (2017) defined r_M values lower than 0.5 as weak connectivity. However, there is no research linking these qualitative descriptions to quantitative estimates beyond the use

of permutation to determine significance (Ambrosini et al. 2009). An additional limitation of r_M values in connectivity profiles is that the spatial connectivity profiles may not be directly relatable to r_M during the wintering period or temporal connectivity because each r_M estimation is derived from locations at a single latitude (i.e. longitudinal variation only). We recommend future research focus on linking r_M values to population implications.

Studying migratory connectivity can direct conservation action through formal evaluation of potential causes of differential population trends (Wilson et al. 2011, Rushing et al. 2016, Hallworth et al. unpubl.). Potential causes associated with places and times of elevated connectivity can be quantitatively tested by deriving meaningful covariates at those places and times (e.g. % habitat loss at stopover areas) and using those covariates to partition variance in breeding ground demographics. Rushing et al. (2016) introduced this approach by modelling the effect of breeding and wintering ground conditions on wood thrush *Hylocichla mustelina* breeding abundance at the population level. Connectivity profiles could extend this approach by narrowing the potential covariates included to just those of places and times of peak or high connectivity, facilitating the inclusion of covariates for the migratory period, and measuring covariates at the individual level. Temporal connectivity profiles enable the inclusion of potential threats that vary with time in the full annual cycle study of differential population trends. Future conservation research for the common nighthawk and other species with similar broad-scale, differential population trends could use this retrospective approach to assess potential threats associated with the places and times of high connectivity identified here.

Conservation of migratory species should be conducted in the context of the full annual cycle (Marra et al. 2015). Authors have used migratory connectivity to investigate differential population trends by focusing on specific places or times during the annual cycle, with particular focus on the wintering grounds (Fraser et al. 2012, Taylor and Stutchbury 2016, Murray et al. 2017, Kramer et al. 2018). Such hypothesis-driven approaches may fail to identify places and times during the annual cycle that limit populations because they do not encompass the full migratory path(s) and often lack a temporal perspective. Our approach provides a comprehensive alternative that also enables, for the first time, evaluation of temporal connectivity. Connectivity profiles can help direct conservation assessment of specific places and times of the annual cycle for the common nighthawk and other migratory species of conservation concern.

Data availability statement

Data are under embargo and will be available from MoveBank in 2022.

Acknowledgements – Our sincere thanks to the many volunteers who assisted with deployment of tags on common nighthawks across North America. Thanks to Mike van den Tillaart at Lotek Wireless for insight and assistance with the PinPoint GPS-Argos tags, to Peter Thomas for coordinating New Brunswick deployments, and to Péter Sólymos for advice on the leave-one-out analysis.

Funding – Data collection funding for this project was generously provided by the Conoco Phillips Global Signature Programs to the Migratory Connectivity Project, Environment and Climate Change Canada, and the Natural Sciences and Engineering Research Council of Canada. Field work funding for this project was provided by Environment and Climate Change Canada, Birds Canada, Texas Tech University, Wendy Bragg, Roger Dietrich, Amber Furness, Paige Oboikovitz ECK was funded by the Natural Sciences and Engineering Research Council of Canada, the University of Alberta, the Killam Foundation, the Canadian Federation of University Women, the Alberta Chapter of the Wildlife Society and the Kay Ball Memorial Graduate Student Research Travel Award.

Permits – Animal capture and tag deployment was conducted under Animal Care and Use Protocols (University of Alberta: AUP00001523; National Zoological Park and Conservation Biology: 15-16, 18-66; Texas Tech University: 15032-04; University of South Dakota: 23-05-13-16C, 15-05-16-19C; Environment and Climate Change SFCQ2017-02), US Federal Bird Banding Permits (09700, 22199, 22834) and Environment and Climate Change Canada Scientific Permit to Capture and Band Migratory Birds (10277, 10365, 10619H, 10534, 10169, 10887). Regional permits were obtained where necessary; details are available upon request.

Author contributions

Elly C. Knight: Conceptualization (lead); Data curation (lead); Formal analysis (lead); Investigation (equal); Methodology (lead); Project administration (lead); Visualization (lead); Writing – original draft (lead). **Autumn-Llynn Harrison**: Conceptualization (supporting); Data curation (supporting); Formal analysis (supporting); Funding acquisition (supporting); Methodology (supporting); Project administration (supporting); Writing – original draft (supporting); Writing – review and editing (equal). **Amy L. Scarpignato**: Conceptualization (supporting); Data curation (supporting); Funding acquisition (supporting); Investigation (equal); Project administration (supporting); Writing – review and editing (equal). **Steven L. Van Wilgenburg**: Conceptualization (supporting); Formal analysis (supporting); Funding acquisition (lead); Methodology (supporting); Supervision (equal); Writing – review and editing (equal). **Erin M. Bayne**: Conceptualization (supporting); Formal analysis (supporting); Funding acquisition (lead); Methodology (supporting); Resources (equal); Supervision (equal); Writing – review and editing (equal). **Janet W. Ng**: Data curation (supporting); Investigation (equal); Project administration (supporting); Writing – review and editing (equal). **Emily Angell**: Investigation (equal); Resources (equal); Writing – review and editing (equal). **R. Bowman**: Investigation (equal); Resources (equal); Writing – review and editing (equal). **R. Mark Brigham**: Methodology (equal); Supervision (equal); Writing – review and editing (equal). **Bruno Drolet**: Investigation (equal); Resources (equal); Writing – review and editing (equal). **Wendy E. Easton**: Investigation (equal); Resources

(equal); Writing – review and editing (equal). **Timothy R. Forrester**: Investigation (equal); Resources (equal); Writing – review and editing (equal). **Jeffrey T. Foster**: Investigation (equal); Resources (equal); Writing – review and editing (equal). **Samuel Haché**: Investigation (equal); Resources (equal); Writing – review and editing (equal). **Kevin C. Hannah**: Investigation (equal); Resources (equal); Writing – review and editing (equal). **Kristina G. Hick**: Investigation (equal); Resources (equal); Writing – review and editing (equal). **Jacques Ibarzabal**: Investigation (equal); Resources (equal); Writing – review and editing (equal). **Tara L. Imlay**: Investigation (equal); Resources (equal); Writing – review and editing (equal). **Stuart A. Mackenzie**: Investigation (equal); Resources (equal); Writing – review and editing (equal). **Alan Marsh**: Investigation (equal); Resources (equal); Writing – review and editing (equal). **Liam P. McGuire**: Investigation (equal); Resources (equal); Writing – review and editing (equal). **Gretchen N. Newberry**: Investigation (equal); Resources (equal); Writing – review and editing (equal). **David Newstead**: Investigation (equal); Resources (equal); Writing – review and editing (equal). **Andrea Sidler**: Investigation (equal); Resources (equal); Writing – review and editing (equal). **Pam H. Sinclair**: Investigation (equal); Resources (equal); Writing – review and editing (equal). **Jaime Stephens**: Investigation (equal); Resources (equal); Writing – review and editing (equal). **David L. Swanson**: Investigation (equal); Resources (equal); Writing – review and editing (equal). **Junior Tremblay**: Investigation (equal); Resources (equal); Writing – review and editing (equal). **Peter P. Marra**: Conceptualization (lead); Formal analysis (supporting); Funding acquisition (lead); Methodology (supporting); Project administration (supporting); Supervision (equal); Writing – review and editing (equal).

References

Åkesson, S. et al. 2012. Migration routes and strategies in a highly aerial migrant, the common swift *Apus apus*, revealed by light-level geolocators. – PLoS One 7: e41195.

Alerstam, T. and Hedenström, A. 1998. The development of bird migration theory. J. Avian Biol. 29: 343–369.

Ambrosini, R. et al. 2009. A quantitative measure of migratory connectivity. – J. Theor. Biol. 257: 203–211.

Bates, D. et al. 2015. Fitting linear mixed-effects models using lme4. – J. Stat. Softw. 67: 1–48.

Bauer, S. et al. 2016. Timing is crucial for consequences of migratory connectivity. – Oikos 125: 605–612.

Bayly, N. J. et al. 2018. Major stopover regions and migratory bottlenecks for Nearctic-Neotropical landbirds within the Neotropics: a review. – Bird Conserv. Int. 28: 1–26.

Borchers, H. W. 2019. Pracma: practical numerical math functions. – R package ver. 2.2.9. <https://cran.r-project.org/web/packages/pracma/index.html>.

Briedis, M. and Bauer, S. 2018. Migratory connectivity in the context of differential migration. – Biol. Lett. 14: 20180679.

Briedis, M. et al. 2016. Breeding latitude leads to different temporal but not spatial organization of the annual cycle in a long-distance migrant. – J. Avian Biol. 47: 743–748.

Brigham, R. M. et al. 2011. Common nighthawk *Chordeiles minor*. – In: Rodewald, P. G. (ed.), Birds of North America. Cornell Lab of Ornithology, Ithaca, NY.

Camacho, C. 2013. Behavioural thermoregulation in man-made habitats: surface choice and mortality risk in red-necked nightjars. – Bird Study 60: 124–130.

Cohen, E. B. et al. 2017a. How do en route events around the Gulf of Mexico influence migratory landbird populations? – Condor 119: 327–343.

Cohen, E. B. et al. 2017b. Quantifying the strength of migratory connectivity. – Methods Ecol. Evol. 85: 749–812.

Cohen, E. B. et al. 2018. The strength of migratory connectivity for birds en route to breeding through the Gulf of Mexico. – Ecography 33: 1035–1112.

Cresswell, W. 2014. Migratory connectivity of Palaearctic–African migratory birds and their responses to environmental change: the serial residency hypothesis. – Ecology 156: 493–510.

Davidson, S. C. et al. 2020. Ecological insights from three decades of animal movement tracking across a changing Arctic. – Science 370: 712–715.

Efron, B. and Stein, C. 1981. The jackknife estimate of variance. – Ann. Stat. 9: 586–596.

English, P. A. et al. 2017. Habitat and food supply across multiple spatial scales influence the distribution and abundance of a nocturnal aerial insectivore. – Landscape Ecol. 32: 343–359.

English, P. A. et al. 2018. Nightjars may adjust breeding phenology to compensate for mismatches between moths and moonlight. – Ecol. Evol. 8: 5515–5529.

Environment Canada. 2016. Recovery strategy for the common nighthawk *Chordeiles minor* in Canada. – Government of Canada.

Finch, T. et al. 2015. A pan-European, multipopulation assessment of migratory connectivity in a near-threatened migrant bird. – Divers. Distrib. 21: 1051–1062.

Finch, T. et al. 2017. Low migratory connectivity is common in long-distance migrant birds. – J. Anim. Ecol. 86: 662– 673.

Fink, D. et al. 2020. eBird status and trends, data ver.: 2018. – Cornell Lab or Ornithology, Ithaca, NY, <https://ebird.org/science/status-and-trends/comnig/abundance-map-weekly>, accessed 26 October 2020.

Fraser, K. C. et al. 2012. Continent-wide tracking to determine migratory connectivity and tropical habitat associations of a declining aerial insectivore. – Proc. R. Soc. B 279: 4901–4906.

Gow, E. A. et al. 2019. A range-wide domino effect and resetting of the annual cycle in a migratory songbird. – Proc. R. Soc. B 286: 20181916-9.

Hijmans, R. J. 2017. geosphere: spherical trigonometry. – R package ver. 1.5-7. <https://cran.r-project.org/package=geosphere>.

Hobson, K. A. et al. 2015. A continent-wide migratory divide in North American breeding barn swallows *Hirundo rustica*. – PLoS One 10: e0129340-13.

Imlay, T. L. et al. 2020. The fall migratory movements of bank swallows, *Riparia riparia*: fly-and-forage migration? – Avian Conserv. Ecol. 15: 2.

Johnson, D. S. and London, J. M. 2018. crawl: an R package for fitting continuous-time correlated random walk models to animal movement data. – Zenodo doi: 10.5281/zenodo.569569

Johnson, D. S. et al. 2008. Continuous-time correlated random walk model for animal telemetry data. – Ecology 89: 1208–1215.

Koleček, J. et al. 2016. Cross-continental migratory connectivity and spatiotemporal migratory patterns in the great reed warbler. – J. Avian Biol. 47: 756–767.

Kramer, G. R. et al. 2018. Population trends in vermivore warblers are linked to strong migratory connectivity. – Proc. Natl Acad. Sci. USA 115: E3192–E3200.
Kranstauber, B. et al. 2011. The Movebank data model for animal tracking. – Environ. Model. Softw. 26: 834–835.
Krzywinski, M and Altman, N. 2013. Points of significance: error bars. – Nature 10: 921–922.
Lisic, J. 2018. meanShiftR: a computationally efficient mean shift implementation. – R package ver. 0.53. <https://cran.r-project.org/package=meanShiftR>.
Marra, P. P. et al. 2006. Migratory connectivity. – In: Crooks, K. and Muttulingam, S. (eds), Maintaining connections for nature. Oxford Univ. Press, pp. 157–183.
Marra, P. P. et al. 2015. A call for full annual cycle research in animal ecology. – Biol. Lett. 11: 20150552.
Marra, P. P. et al. 2018. Migratory connectivity. – In: Choe, J. (ed.), Encyclopedia of animal behavior, Vol. 2. Oxford Academic Press, pp. 645–654.
Murray, N. J. et al. 2017. The large-scale drivers of population declines in a long-distance migratory shorebird. – Ecography 41: 867–876.
Ng, J. W. et al. 2018. First full annual cycle tracking of a declining aerial insectivorous bird, the common nighthawk *Chordeiles minor*, identifies migration routes, nonbreeding habitat and breeding site fidelity. – Can. J. Zool. 96: 869–875.
Norris, R. and Marra, P. P. 2007. Seasonal interactions, habitat quality and population dynamics in migratory birds. – Condor 109: 535–547.
Phipps, W. L. et al. 2019. Spatial and temporal variability in migration of a soaring raptor across three continents. – Front. Ecol. Evol. 7: 323.
Ries, L. et al. 2018. Flying through hurricane central: impacts of hurricanes on migrants with a focus on monarch butterflies. – Anim. Mig. 5: 94–103.
Rodríguez Eraso, N. et al. 2013. Land use and land cover change in the Colombian Andes: dynamics and future scenarios. – J. Land Use Sci. 8: 154–174.
Rowcliffe, J. M. et al. 2012. Bias in estimating animal travel distance: the effect of sampling frequency. – Methods Ecol. Evol. 3: 653–662.
Rushing, C. S. et al. 2016. Quantifying drivers of population dynamics for a migratory bird throughout the annual cycle. – Proc. R. Soc. B 283: 20152846-10.
Sánchez-Bayo, F. and Wyckhuys, K. A. G. 2019. Worldwide decline of the entomofauna: a review of its drivers. – Biol. Conserv. 232: 8–27.
Sarà, M. et al. 2019. Broad-front migration leads to strong migratory connectivity in the lesser kestrel *Falco naumanni*. – J. Biogeogr. 46: 2663–2677.
Sauer, J. R. et al. 2017. The North American Breeding Bird Survey, results and analysis 1966–2015. Ver.207.2017. – USGS Patuxent Wildlife Research Center.
Scarpignato, A. L. et al. 2016. Field-testing a new miniaturized GPS-Argos satellite transmitter (3.5 g) on migratory shorebirds. – Wader Study 123: 240–246.
Spiller, K. J. and Dettmers, R. 2019. Evidence for multiple drivers of aerial insectivore declines in North America. – Condor 121: 42–53.
Taylor, C. M. and Stutchbury, B. J. M. 2016. Effects of breeding versus winter habitat loss and fragmentation on the population dynamics of a migratory songbird. – Ecol. Appl. 26: 424–437.
van Wijk, R. E. et al. 2018. Diverse migration strategies in hoopoes *Upupa epops* lead to weak spatial but strong temporal connectivity. – Sci. Nat. 105: 42.
Webster, M. S. and Marra, P. P. 2005. The importance of understanding migratory connectivity and seasonal interactions. – In: Greenberg, R. and Marra, P. P. (eds), Birds of two worlds: the ecology and evolution of migration. Johns Hopkins Univ. Press, pp. 199–209.
Webster, M. S. et al. 2002. Links between worlds: unraveling migratory connectivity. – Trends Ecol. Evol. 17: 76–83.
Wilson, S. et al. 2011. Range-wide effects of breeding- and nonbreeding-season climate on the abundance of a Neotropical migrant songbird. – Ecology 92: 1789–1798.
Wood, S. N. 2011. Fast stable restricted maximum likelihood and marginal likelihood estimation of semiparametric generalized linear models. – J. R. Stat. Soc. B 73: 3–36.
Wood, S. N. 2017. Generalized additive models: an introduction with R, 2nd edn. – CRC Press.